

# Search for dark matter annihilation line signals with the H.E.S.S. Inner Galaxy Survey

**Emmanuel Moulin<sup>a,\*</sup> and Alessandro Montanari<sup>b</sup> on behalf of the H.E.S.S. collaboration**

<sup>a</sup>*IRFU, CEA, Université Paris-Saclay, F-91191 Gif-sur-Yvette, France*

<sup>b</sup>*Landessternwarte, Universität Heidelberg, Königstuhl, D 69117 Heidelberg, Germany*

*E-mail:* [emmanuel.moulin@cea.fr](mailto:emmanuel.moulin@cea.fr), [amontanari@lsw.uni-heidelberg.de](mailto:amontanari@lsw.uni-heidelberg.de)

Astrophysical and cosmological measurements suggest that non-baryonic dark matter dominates the matter content of the Universe. However, its underlying nature remains elusive. Among the most promising candidates are weakly interacting massive particles (WIMPs): particles with mass and coupling strength at the electroweak scale and thermally produced in the early universe having a present relic density consistent with that observed today. WIMP self-annihilation could produce Standard Model particles, including gamma-rays, which have been long-time recognized as a prime messenger to indirectly detect dark matter signals. Line-like features expected in the gamma-ray spectra from WIMP self-annihilation provide a key signature for TeV-scale particle dark matter. The centre of the Milky Way is predicted as the brightest source of DM annihilations. The H.E.S.S. collaboration is currently performing a survey of the inner region of the Milky Way, the Inner Galaxy Survey (IGS). We analyzed 2014-2020 observations taken with the five-telescope array to search for a DM line annihilation signal. With the current dataset of 546 hours, we found no significant excess and therefore derived strong constraints on the velocity-weighted annihilation cross-section into two gammas. Our limits significantly improve the current constraints, opening the possibility of constraining canonical thermal Dark Matter models with prominent line contribution in their annihilation spectra, as expected in the Wino and Higgsino cases.

POS( ICRC2023 ) 1424

38th International Cosmic Ray Conference (ICRC2023)  
26 July - 3 August, 2023  
Nagoya, Japan



---

\*Speaker

## 1. Dark Matter signatures in gamma-ray observations

The hypothesis that 85% of the total matter content of the Universe is made of a dark and non-baryonic component is validated by several astrophysical and cosmological measurements [1]. Many theories beyond the Standard Model have attempted an explanation of this dark matter (DM), and among the most compelling candidates for stable DM are weakly interacting massive particles (WIMPs), with mass and coupling strength at the electroweak scale [2–4]. When WIMPs are considered thermally produced in the early Universe, they can constitute all the DM in the Universe [5]. The search for WIMPs motivated a plethora of experiments [6, 7], many of which aiming at the detection of what is produced from WIMPs decay and annihilation [8]. Self-annihilation of WIMPs could happen in dense astrophysical environments. Very-high-energy (VHE,  $E \gtrsim 100$  GeV)  $\gamma$ -rays from hadronization, radiation, and decay of standard model particles could be produced in the final state. If the WIMP mass is large enough, the  $\gamma$ -rays obtained from annihilation could be detected by the H.E.S.S. array of five Imaging Atmospheric Cherenkov Telescopes (IACTs).

The energy-differential flux of gamma-rays from self-annihilation of Majorana WIMPs can be expressed as:

$$\frac{d\Phi_\gamma}{dE_\gamma}(E_\gamma, \Delta\Omega) = \frac{\langle\sigma v\rangle}{8\pi m_{\text{DM}}^2} \sum_f BR_f \frac{dN^f}{dE_\gamma}(E_\gamma) J(\Delta\Omega)$$

with  $J(\Delta\Omega) = \int_{\Delta\Omega} \int_{\text{los}} \rho^2(s(r, \theta)) ds d\Omega$ . (1)

This considers the flux in a solid angle  $\Delta\Omega$ . The velocity-weighted annihilation cross-section averaged over the velocity distribution is given by  $\langle\sigma v\rangle$ . The differential gamma-ray yield is expressed with  $dN^f/dE_\gamma$ , per annihilation in the channel  $f$  with branching ratio  $BR_f$ . The J-factor  $J(\Delta\Omega)$ , is computed with the integral of the square of the DM density  $\rho$  over the line of sight (los)  $s$  and the solid angle  $\Delta\Omega$ . For this work,  $\rho$  is assumed spherically symmetric. Therefore, the J-factor depends only on the radial coordinate  $r$  from the center of the DM halo, which can be simplified to  $r = (s^2 + r_\odot^2 - 2r_\odot s \cos\theta)^{1/2}$ , where the distance between the observer and the GC is fixed to  $r_\odot = 8.5$  kpc [9], and the angle between the direction of the observation and the Galactic Center (GC) is  $\theta$ . A common assumption for the DM distribution in the GC is that it follows a cuspy profile, often described by the NFW [10] and Einasto [11] parametrizations. With these premises, the centre of the Milky Way is predicted as the brightest source of DM annihilation signal.

A continuum spectrum of  $\gamma$ -rays up to the DM mass  $m_{\text{DM}}$  is expected from prompt self-annihilation of WIMPs into quarks, heavy leptons, or gauge bosons which eventually hadronize and/or decay. The DM self-annihilation at rest into  $\gamma X$ , being  $X = \gamma, H, Z$  or a non Standard Model neutral particle, would result in a distinguishable and narrow spectral line at  $E_\gamma = m_{\text{DM}}(1 - m_X^2/4m_{\text{DM}}^2)$ . This is limited by the resolution of the detector, given that the relative velocity of the DM particles is low ( $\sim 10^{-3}c$ ). Moreover, DM self-annihilation into charged particles would produce additional  $\gamma$  rays from final state radiation and virtual internal bremsstrahlung, which justify bumpy bremsstrahlung features and, therefore, a wider line peaking at an energy close to  $m_{\text{DM}}$ . The process of DM prompt annihilation into two photons is loop-suppressed compared to the continuum one because it cannot take place at tree level. However, it gives the clearest signature

of DM annihilation. The strongest constraints on the continuum signal were obtained, so far, with the 546 hours of the H.E.S.S. Inner Galaxy Survey observational program of the GC [12]. The strongest constraints on the annihilation of DM into two photons were obtained with 254 hours of H.E.S.S. observations [13] and 223 hours of MAGIC observations [14] of the GC.

The left panel of Fig. 1 shows the expected gamma-ray yield per annihilation in various annihilation channels for DM masses of 1 and 10 TeV, respectively. The spectrum resulting from DM prompt annihilation into two photons is convolved by a Gaussian function of width  $\sigma/E = 10\%$ , representing the energy resolution of the H.E.S.S. instrument. The J-factor map computed for a DM distribution following the Einasto density profile parametrization, extracted from Ref. [12], is shown on the right panel of Fig. 1.

In this work, we show new constraints on the cross section for DM self-annihilation into two gammas. Moreover, we compare our derived limits to theoretical line cross section predictions for canonical TeV DM models for which prominent line contribution in the annihilation spectra, like the Wino and Higgsino [15], are expected. The latter models produce the correct DM abundance, when enclosed in a thermal relic cosmology, if their masses are fixed to  $2.9 \pm 0.1$  TeV and  $1.0 \pm 0.1$  TeV, respectively [16–18].

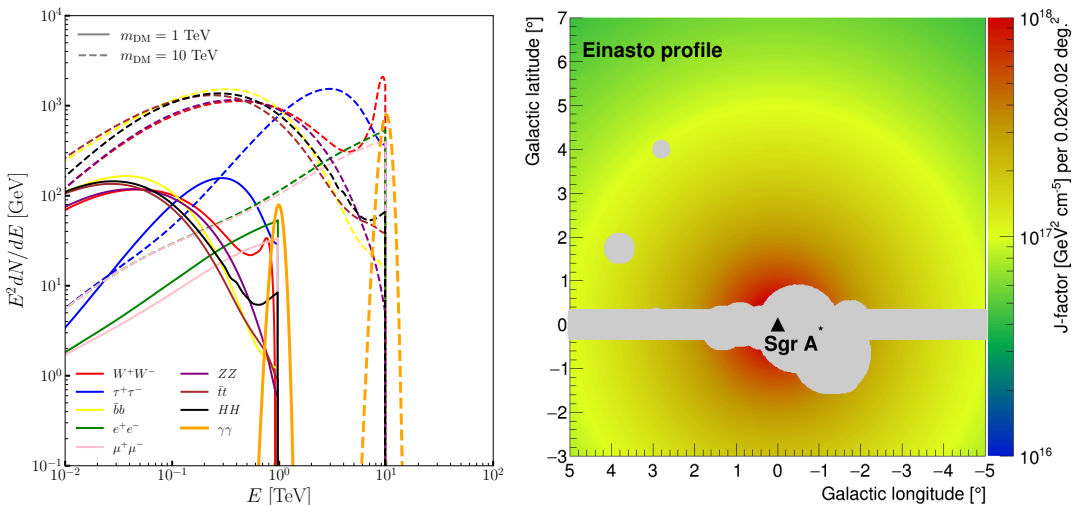


**Figure 1:** *Left:* Gamma-ray annihilation spectrum versus energy in the  $W^+W^-$ ,  $\tau^+\tau^-$ ,  $b\bar{b}$ ,  $\mu^+\mu^-$ ,  $e^+e^-$ ,  $ZZ$ ,  $t\bar{t}$ ,  $HH$ , and  $\gamma\gamma$  annihilation channels for DM masses of 1 and 10 TeV, respectively. The spectrum for the  $\gamma\gamma$  annihilation channel is convolved by a Gaussian function of width  $\sigma/E = 10\%$ . *Right:* J-factor map in Galactic coordinates for the DM distribution in the Milky Way following an Einasto profile [12]. The grey-shaded area shows the conservative set of masks adopted in the analysis [12].

## 2. Observations and data analysis

The data used here consist of 546 hours of high-quality observations taken during the Inner Galaxy Survey carried out by H.E.S.S. from 2014 to 2020. The data analysis is performed in regions of interest (ROI) defined by concentric annuli of  $0.1^\circ$  width centered on the GC, with inner radii from  $0.5^\circ$  up to  $2.9^\circ$ . The known astrophysical sources in the whole field of view of the IGS

observations are masked in order to avoid gamma-ray contamination in the ROI and the challenging modelling of these emissions. We use the same conservative set of masks as in Ref. [12]. These masks are shown in the right panel of Fig. 1. The residual gamma-ray background measurement is performed for each observational run in an OFF region taken symmetrically to the ON region from the pointing position of the run. The masked regions are removed alike in the ON and OFF regions such that these regions have the same acceptance and field of view.

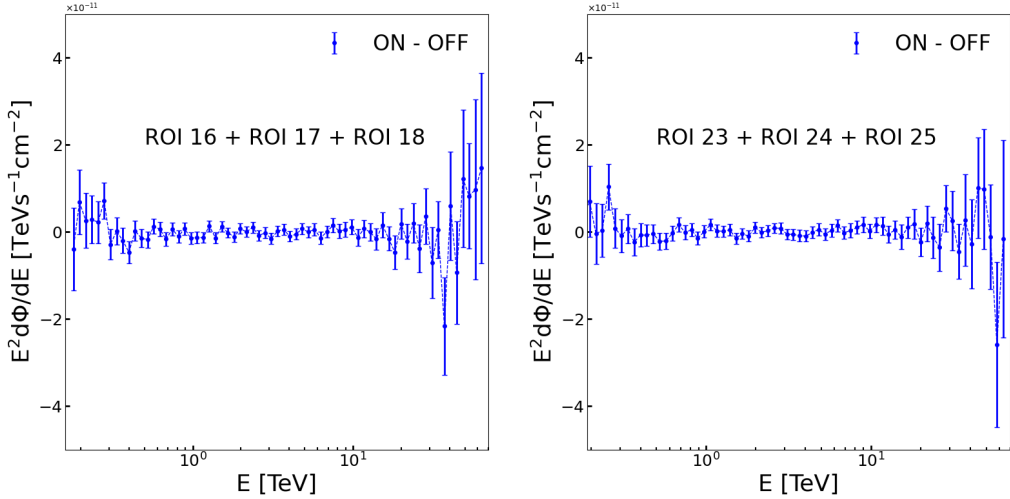


**Figure 2:** Background-subtracted energy-differential flux multiplied by  $E^2$  versus energy for the combinations of ROIs 16, 17 and 18 (left panel) and ROIs 23, 24, 25 (right panel).  $1\sigma$  error bars are shown.

The data analysis is performed with a 2-dimensional log-likelihood ratio test statistics (TS) using the spectral and spatial features of the search DM line signal in 67 logarithmically spaced energy bins and 25 spatial bins, the latter corresponding to the above-mentioned 25 ROIs. The likelihood function writes as:

$$\mathcal{L}_{ij}(\mathbf{N}^S, \mathbf{N}^B | \mathbf{N}_{ON}, \mathbf{N}_{OFF}) = \frac{[\beta_{ij}(N_{ij}^S + N_{ij}^B)]^{N_{ON,ij}}}{N_{ON,ij}!} e^{-\beta_{ij}(N_{ij}^S + N_{ij}^B)} \frac{[\beta_{ij}(N_{ij}^{S'} + N_{ij}^B)]^{N_{OFF,ij}}}{N_{OFF,ij}!} e^{-\beta_{ij}(N_{ij}^{S'} + N_{ij}^B)} e^{-\frac{(1-\beta_{ij})^2}{2\sigma_{\beta_{ij}}^2}}. \quad (2)$$

$N_{ij}^S$  and  $N_{ij}^{S'}$  are the number of expected signal count in the  $(i, j)$  bin of the ON and OFF regions, respectively. They are obtained by folding the expected DM flux given in Eq. (1) with the energy-dependent acceptance and energy resolution. The J-factor values are computed for each ROI.  $N_{ij}^B$  is the expected number of background events in the  $(i, j)$  for the ON and OFF regions.  $N_{ON,ij}$  and  $N_{OFF,ij}$  are the number of measured event in the ON and OFF regions, respectively. The systematic uncertainty can be introduced in the likelihood function as a Gaussian nuisance parameter where  $\beta_{ij}$  is a normalization factor and  $\sigma_{\beta_{ij}}$  is the width of the Gaussian function (see, for instance, Refs. [12, 19–21]). Maximizing the likelihood function such that  $dL_{ij}/d\beta_{ij} \equiv 0$  allows us to derive  $\beta_{ij}$ , using  $\sigma_{\beta_{ij}} = 1\%$  [12].

No significant excess compatible with the searched DM line signal is found in any of the ON regions with respect to the OFF regions. Therefore, constraints on  $\langle \sigma v \rangle_{\text{line}}$  are obtained from the log-likelihood ratio TS described in Ref. [22] assuming a positive signal  $\langle \sigma v \rangle_{\text{line}} > 0$ . We used the

high statistics limit in which the TS follows a  $\chi^2$  distribution with one degree of freedom.  $\langle\sigma v\rangle_{\text{line}}$  values for which TS is higher than 2.71 are excluded at the 95% confidence level (C.L.). The expected limits are computed via the Asimov procedure [22] which provides a good agreement with the Monte Carlo approach generating many realizations of the expected background [21].

### 3. Results

The left panel of Fig. 3 shows the constraints obtained with the 2014-2020 H.E.S.S. IGS observations. The constraints are given in terms of 95% C.L. upper limits on the velocity-weighted annihilation line cross-section  $\langle\sigma v\rangle_{\text{line}}$  as a function of the DM mass  $m_{\text{DM}}$ . They reach  $2.4 \times 10^{-28}$  and  $2.9 \times 10^{-27} \text{ cm}^3 \text{s}^{-1}$  for DM masses of 1 and 10 TeV, respectively. The mean expected limits are given together with the 68% and 95% C.L. statistical containment bands. They are also shown when the systematic uncertainty is included in the likelihood function as explained above. The sensitivity reached in this work allows us to be able to probe  $\langle\sigma v\rangle_{\text{line}}$  values expected for thermal-relic WIMPs.

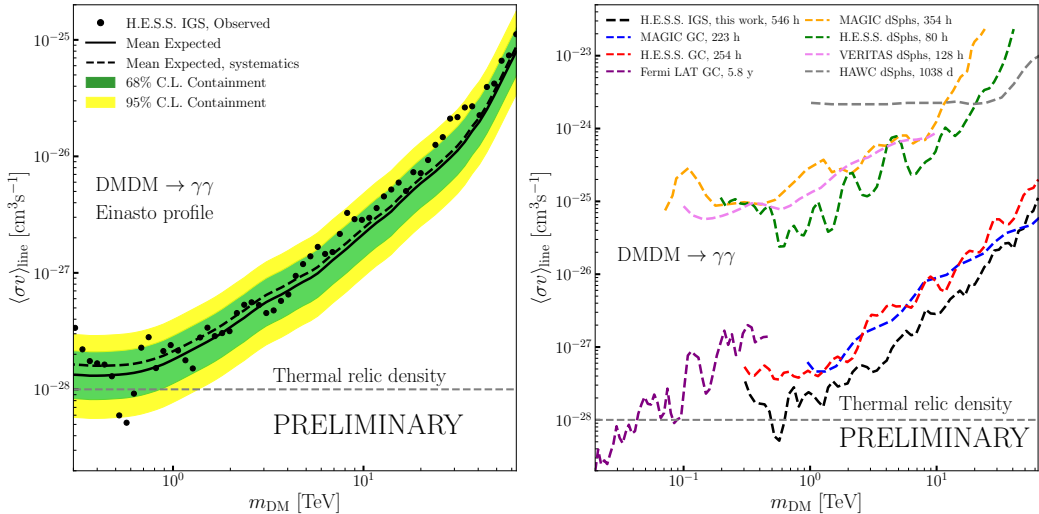


**Figure 3:** *Left:* 95% C. L. upper limits on the velocity-weighted annihilation line cross section  $\langle\sigma v\rangle_{\text{line}}$  as function of the DM mass  $m_{\text{DM}}$  using the H.E.S.S. IGS observations from 2014 to 2020. The observed limits are shown as black dots. The mean expected limits (black solid line) together with the 68% (green band) and 95% (yellow band) C.L. statistical containment bands are also shown. The mean expected upper limit with systematic uncertainty is also shown (black dashed line). *Right:* Current constraints on the velocity-weighted annihilation line cross section  $\langle\sigma v\rangle_{\text{line}}$  as function of the DM mass  $m_{\text{DM}}$  including previous H.E.S.S. limits from 254 h of observations of the GC [13] (red line), the limits from 223 h of GC observations with MAGIC [14] (blue line), and the limits from 5.8 y of observations of the GC with the Fermi satellite [23] (purple line). The limits from the dwarf spheroidal galaxy observations with HAWC [24] (grey line), H.E.S.S. [25] (green line), MAGIC [26] (yellow line) and VERITAS [27] (pink line) are also shown. The natural scale for monochromatic gamma-ray line signal from DM annihilations is shown as a gray-shaded area.

The right panel of Fig. 3 shows a comparison of the limits obtained in this work with the 2018 H.E.S.S. constraints from 254 hours of observation of the GC [13], the current constraints from 223

hours of GC observations by MAGIC [14], and the Fermi-LAT [23] constraints from 5.8 years of observations of the GC. In addition, the limits obtained by HAWC [24], H.E.S.S. [25], MAGIC [26] and VERITAS [27] from dwarf spheroidal galaxy observations are shown. The limits obtained in this work are the strongest so far for DM masses above 300 GeV. They well complement the limits obtained by Fermi-LAT in the 20 GeV - 300 GeV mass range.

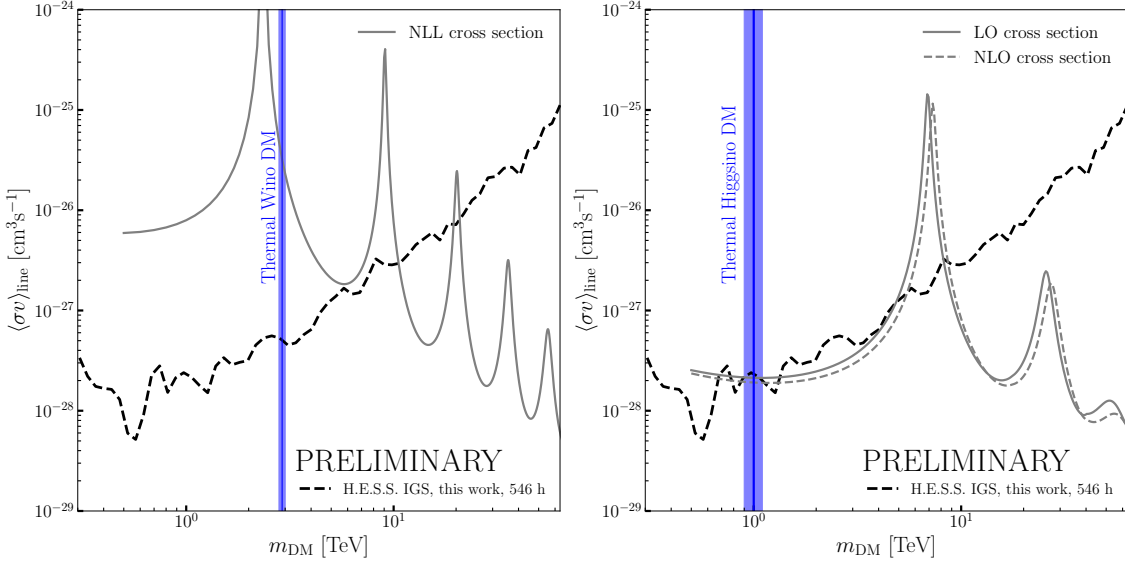


**Figure 4:** 95% C. L. upper limits on the velocity-weighted annihilation line cross section  $\langle\sigma v\rangle_{\text{line}}$  (black dashed line) as function of the DM mass  $m_{\text{DM}}$ . *Left:* The limits are compared to the theoretical prediction for the Wino cross-section [16] obtained with next-to-leading logarithmic computation (grey line). The blue line shows the value of the Wino mass to obtain the correct relic abundance when considering a thermal cosmology. *Right:* The same comparison is shown for the theoretical prediction for the Higgsino cross section [17, 30] given for both the leading-order (grey solid line) and next-to-leading logarithmic (grey dashed line) computations, respectively. The blue line shows the value of the Higgsino mass to obtain the correct relic abundance when considering a thermal cosmology.

Figure 4 shows the comparison between the limits obtained in this work and the theoretical predictions for the annihilation cross sections for the canonical TeV DM models of the Wino [28, 29] and Higgsino [17, 30].

#### 4. Summary

The data set obtained with the IGS observational program performed by H.E.S.S. has been analyzed to look for DM-line signatures. No significant excess compatible with the searched DM signal is observed in the region of interest covering the inner  $3^\circ$  of the Milky Way. The limits have been derived on the thermally-averaged velocity-weighted annihilation cross section of DM particles annihilating into two photons. The mean expected upper limits improve over the previous H.E.S.S. limits by a factor of around 2.2 for a DM mass of 1 TeV. The limits reached in this work are the strongest so far in the 300 GeV - 50 TeV mass range.

The limits obtained in this work are confronted to predictions in the framework of canonical TeV DM models, such as the Wino and the Higgsino, where a prominent line contribution is predicted

in the final-state gamma-ray spectrum. The limits obtained in this work exclude the thermal Wino model. The current limits challenge the thermal Higgsino model for the theoretical assumptions adopted in this work. H.E.S.S. is still collecting data towards the GC region. Therefore, a larger dataset would push the constraints even further.

## References

- [1] R. Adam *et al.* [Planck Coll.], Astron. Astrophys. **594** (2016), A1 [arXiv:1502.01582 [astro-ph.CO]].
- [2] G. Bertone, J. Silk, B. Moore, *et al.* Cambridge Univ. Press, 2010, ISBN 978-1-107-65392-4
- [3] J. L. Feng, Ann. Rev. Astron. Astrophys. **48** (2010), 495-545 [arXiv:1003.0904 [astro-ph.CO]].
- [4] L. Roszkowski, E. M. Sessolo and S. Trojanowski, Rept. Prog. Phys. **81** (2018) no.6, 066201 [arXiv:1707.06277 [hep-ph]].
- [5] G. Jungman, M. Kamionkowski and K. Griest, Phys. Rept. **267** (1996), 195-373 [arXiv:hep-ph/9506380 [hep-ph]].
- [6] F. Kahlhoefer, Int. J. Mod. Phys. A **32** (2017) no.13, 1730006 [arXiv:1702.02430 [hep-ph]].
- [7] M. Schumann, J. Phys. G **46** (2019) no.10, 103003 [arXiv:1903.03026 [astro-ph.CO]].
- [8] L. E. Strigari, Rept. Prog. Phys. **81** (2018) no.5, 056901 [arXiv:1805.05883 [astro-ph.CO]].
- [9] A. M. Ghez, S. Salim, N. N. Weinberg, *et al.*, Astrophys. J. **689** (2008) [arXiv:0808.2870 [astro-ph]].
- [10] J. F. Navarro, C. S. Frenk and S. D. M. White, Astrophys. J. **490** (1997), 493-508 [arXiv:astro-ph/9611107 [astro-ph]].
- [11] V. Springel, S. D. M. White, C. S. Frenk, *et al.*, Nature 456 (2008) 73 [arXiv:0809.0894 [astro-ph]].
- [12] H. Abdalla *et al.* [H.E.S.S. Coll.], Phys. Rev. Lett. **129** (2022) no.11, 111101 [arXiv:2207.10471 [astro-ph.HE]].
- [13] H. Abdallah *et al.* [H.E.S.S. Coll.], Phys. Rev. Lett. **120** (2018) no.20, 201101 [arXiv:1805.05741 [astro-ph.HE]].
- [14] H. Abe *et al.* [MAGIC Coll.], Phys. Rev. Lett. **130** (2023) no.6, 061002 [arXiv:2212.10527 [astro-ph.HE]].
- [15] M. Cirelli, T. Hambye, P. Panci, F. Sala and M. Taoso, JCAP **10** (2015), 026 [arXiv:1507.05519 [hep-ph]].
- [16] M. Baumgart, T. Cohen, I. Moult, *et al.*, JHEP **03** (2018), 117 [arXiv:1712.07656 [hep-ph]].

- [17] M. Beneke, C. Hasner, K. Urban and M. Vollmann, JHEP **03** (2020), 030 [arXiv:1912.02034 [hep-ph]].
- [18] S. Bottaro, D. Buttazzo, M. Costa, R. Franceschini, P. Panci, D. Redigolo and L. Vittorio, Eur. Phys. J. C **82** (2022) no.1, 31 [arXiv:2107.09688 [hep-ph]].
- [19] V. Lefranc, E. Moulin, P. Panci and J. Silk, Phys. Rev. D **91** (2015) no.12, 122003 [arXiv:1502.05064 [astro-ph.HE]].
- [20] E. Moulin, J. Carr, J. Gaskins, M. Doro, C. Farnier, M. Wood and H. Zechlin, in Science with the Cherenkov Telescope Array (World Scientific, Singapore, 2019), pp. 45–81,
- [21] A. Montanari, E. Moulin and N. L. Rodd, Phys. Rev. D **107** (2023) no.4, 043028 [arXiv:2210.03140 [astro-ph.HE]].
- [22] G. Cowan, K. Cranmer, E. Gross and O. Vitells, Eur. Phys. J. C **71** (2011), 1554 [erratum: Eur. Phys. J. C **73** (2013), 2501] [arXiv:1007.1727 [physics.data-an]].
- [23] M. Ackermann *et al.* [Fermi-LAT Coll.], Phys. Rev. D **91** (2015) no.12, 122002 [arXiv:1506.00013 [astro-ph.HE]].
- [24] A. Albert *et al.* [HAWC Coll.], Phys. Rev. D **101** (2020) no.10, 103001 [arXiv:1912.05632 [astro-ph.HE]].
- [25] H. Abdallah *et al.* [H.E.S.S. Coll.], Phys. Rev. D **102** (2020) no.6, 062001 [arXiv:2008.00688 [astro-ph.HE]].
- [26] V. A. Acciari *et al.* [MAGIC Coll.], Phys. Dark Univ. **35** (2022), 100912 [arXiv:2111.15009 [astro-ph.HE]].
- [27] S. Archambault *et al.* [VERITAS Coll.], Phys. Rev. D **95** (2017) no.8, 082001 [arXiv:1703.04937 [astro-ph.HE]].
- [28] L. Rinchiuso, N. L. Rodd, I. Moult, E. Moulin, M. Baumgart, T. Cohen, T. R. Slatyer, I. W. Stewart and V. Vaidya, Phys. Rev. D **98** (2018) no.12, 123014 [arXiv:1808.04388 [astro-ph.HE]].
- [29] M. Baumgart, T. Cohen, E. Moulin, I. Moult, L. Rinchiuso, N. L. Rodd, T. R. Slatyer, I. W. Stewart and V. Vaidya, JHEP **01** (2019), 036 [arXiv:1808.08956 [hep-ph]].
- [30] L. Rinchiuso, O. Macias, E. Moulin, N. L. Rodd and T. R. Slatyer, Phys. Rev. D **103** (2021) no.2, 023011 [arXiv:2008.00692 [astro-ph.HE]].

## H.E.S.S. author list

F. Aharonian<sup>1,2,3</sup>, F. Ait Benkhali<sup>4</sup>, A. Alkan<sup>5</sup>, J. Aschersleben<sup>6</sup>, H. Ashkar<sup>7</sup>, M. Backes<sup>8,9</sup>, A. Baktash<sup>10</sup>, V. Barbosa Martins<sup>11</sup>, A. Barnacka<sup>12</sup>, J. Barnard<sup>13</sup>, R. Batzofin<sup>14</sup>, Y. Becherini<sup>15,16</sup>, G. Beck<sup>17</sup>, D. Berge<sup>11,18</sup>, K. Bernlöhr<sup>2</sup>, B. Bi<sup>19</sup>, M. Böttcher<sup>9</sup>, C. Boisson<sup>20</sup>, J. Bolmont<sup>21</sup>, M. de Bony de Lavergne<sup>5</sup>, J. Borowska<sup>18</sup>, M. Bouyahaoui<sup>2</sup>, F. Bradascio<sup>5</sup>, M. Breuhaus<sup>2</sup>, R. Brose<sup>1</sup>, A. Brown<sup>22</sup>, F. Brun<sup>5</sup>, B. Bruno<sup>23</sup>, T. Bulik<sup>24</sup>, C. Burger-Scheidlin<sup>1</sup>, T. Bylund<sup>5</sup>, F. Cangemi<sup>21</sup>, S. Caroff<sup>25</sup>, S. Casanova<sup>26</sup>, R. Cecil<sup>10</sup>, J. Celic<sup>23</sup>, M. Cerruti<sup>15</sup>, P. Chambery<sup>27</sup>, T. Chand<sup>9</sup>, S. Chandra<sup>9</sup>, A. Chen<sup>17</sup>, J. Chibueze<sup>9</sup>, O. Chibueze<sup>9</sup>, T. Collins<sup>28</sup>, G. Cotter<sup>22</sup>, P. Cristofari<sup>20</sup>, J. Damascene Mbarubucyeye<sup>11</sup>, I.D. Davids<sup>8</sup>, J. Davies<sup>22</sup>, L. de Jonge<sup>9</sup>, J. Devin<sup>29</sup>, A. Djannati-Ataï<sup>15</sup>, J. Djuvslund<sup>2</sup>, A. Dmytricov<sup>9</sup>, V. Doroshenko<sup>19</sup>, L. Dreyer<sup>9</sup>, L. Du Plessis<sup>9</sup>, K. Egberts<sup>14</sup>, S. Einecke<sup>28</sup>, J.-P. Ernenwein<sup>30</sup>, S. Fegan<sup>7</sup>, K. Feijen<sup>15</sup>, G. Fichet de Clairfontaine<sup>20</sup>, G. Fontaine<sup>7</sup>, F. Lott<sup>8</sup>, M. Füßling<sup>11</sup>, S. Funk<sup>23</sup>, S. Gabici<sup>15</sup>, Y.A. Gallant<sup>29</sup>, S. Ghafourizadeh<sup>4</sup>, G. Giavitto<sup>11</sup>, L. Giunti<sup>15,5</sup>, D. Glawion<sup>23</sup>, J.F. Glicenstein<sup>5</sup>, J. Glombitzka<sup>23</sup>, P. Goswami<sup>15</sup>, G. Grolleron<sup>21</sup>, M.-H. Grondin<sup>27</sup>, L. Haerer<sup>2</sup>, S. Hattingh<sup>9</sup>, M. Haupt<sup>11</sup>, G. Hermann<sup>2</sup>, J.A. Hinton<sup>2</sup>, W. Hofmann<sup>2</sup>, T. L. Holch<sup>11</sup>, M. Holler<sup>31</sup>, D. Horns<sup>10</sup>, Zhiqiu Huang<sup>2</sup>, A. Jaitly<sup>11</sup>, M. Jamrozy<sup>12</sup>, F. Jankowsky<sup>4</sup>, A. Jardin-Blicq<sup>27</sup>, V. Joshi<sup>23</sup>, I. Jung-Richardt<sup>23</sup>, E. Kasai<sup>8</sup>, K. Katarzyński<sup>32</sup>, H. Katjaita<sup>8</sup>, D. Khangulyan<sup>33</sup>, R. Khatoon<sup>9</sup>, B. Khélifi<sup>15</sup>, S. Klepser<sup>11</sup>, W. Kluźniak<sup>34</sup>, Nu. Komin<sup>17</sup>, R. Konno<sup>11</sup>, K. Kosack<sup>5</sup>, D. Kostunin<sup>11</sup>, A. Kundu<sup>9</sup>, G. Lamanna<sup>25</sup>, R.G. Lang<sup>23</sup>, S. Le Stum<sup>30</sup>, V. Lefranc<sup>5</sup>, F. Leitl<sup>23</sup>, A. Lemière<sup>15</sup>, M. Lemoine-Goumard<sup>27</sup>, J.-P. Lenain<sup>21</sup>, F. Leuschner<sup>19</sup>, A. Luashvili<sup>20</sup>, I. Lypova<sup>4</sup>, J. Mackey<sup>1</sup>, D. Malyshev<sup>19</sup>, D. Malyshev<sup>23</sup>, V. Marandon<sup>5</sup>, A. Marcowith<sup>29</sup>, P. Marinos<sup>28</sup>, G. Martí-Devesa<sup>31</sup>, R. Marx<sup>4</sup>, G. Maurin<sup>25</sup>, A. Mehta<sup>11</sup>, P.J. Meintjes<sup>13</sup>, M. Meyer<sup>10</sup>, A. Mitchell<sup>23</sup>, R. Moderski<sup>34</sup>, L. Mohrmann<sup>2</sup>, A. Montanari<sup>4</sup>, C. Moore<sup>35</sup>, E. Moulin<sup>5</sup>, T. Murach<sup>11</sup>, K. Nakashima<sup>23</sup>, M. de Naurois<sup>7</sup>, H. Ndiyavala<sup>8,9</sup>, J. Niemiec<sup>26</sup>, A. Priyana Noel<sup>12</sup>, P. O'Brien<sup>35</sup>, S. Ohm<sup>11</sup>, L. Olivera-Nieto<sup>2</sup>, E. de Ona Wilhelmi<sup>11</sup>, M. Ostrowski<sup>12</sup>, E. Oukacha<sup>15</sup>, S. Panny<sup>31</sup>, M. Panter<sup>2</sup>, R.D. Parsons<sup>18</sup>, U. Pensée<sup>21</sup>, G. Peron<sup>15</sup>, S. Pita<sup>15</sup>, V. Poireau<sup>25</sup>, D.A. Prokhorov<sup>36</sup>, H. Prokopoff<sup>11</sup>, G. Pühlhofer<sup>19</sup>, M. Punch<sup>15</sup>, A. Quirrenbach<sup>4</sup>, M. Regeard<sup>15</sup>, P. Reichherzer<sup>5</sup>, A. Reimer<sup>31</sup>, O. Reimer<sup>31</sup>, I. Reis<sup>5</sup>, Q. Remy<sup>2</sup>, H. Ren<sup>2</sup>, M. Renaud<sup>29</sup>, B. Reville<sup>2</sup>, F. Rieger<sup>2</sup>, G. Roellinghoff<sup>23</sup>, E. Rol<sup>36</sup>, G. Rowell<sup>28</sup>, B. Rudak<sup>34</sup>, H. Rueda Ricarte<sup>5</sup>, E. Ruiz-Velasco<sup>2</sup>, K. Sabri<sup>29</sup>, V. Sahakian<sup>37</sup>, S. Sailer<sup>2</sup>, H. Salzmann<sup>19</sup>, D.A. Sanchez<sup>25</sup>, A. Santangelo<sup>19</sup>, M. Sasaki<sup>23</sup>, J. Schäfer<sup>23</sup>, F. Schüssler<sup>5</sup>, H.M. Schutte<sup>9</sup>, M. Senniappan<sup>16</sup>, J.N.S. Shapogi<sup>8</sup>, S. Shilunga<sup>8</sup>, K. Shiningayamwe<sup>8</sup>, H. Sol<sup>20</sup>, H. Spackman<sup>22</sup>, A. Specovius<sup>23</sup>, S. Spencer<sup>23</sup>, L. Stawarz<sup>12</sup>, R. Steenkamp<sup>8</sup>, C. Stegmann<sup>14,11</sup>, S. Steinmassl<sup>2</sup>, C. Steppa<sup>14</sup>, K. Streil<sup>23</sup>, I. Sushch<sup>9</sup>, H. Suzuki<sup>38</sup>, T. Takahashi<sup>39</sup>, T. Tanaka<sup>38</sup>, T. Tavernier<sup>5</sup>, A.M. Taylor<sup>11</sup>, R. Terrier<sup>15</sup>, A. Thakur<sup>28</sup>, J. H.E. Thiersen<sup>9</sup>, C. Thorpe-Morgan<sup>19</sup>, M. Tluczykont<sup>10</sup>, M. Tsirou<sup>11</sup>, N. Tsuji<sup>40</sup>, R. Tuffs<sup>2</sup>, Y. Uchiyama<sup>33</sup>, M. Ullmo<sup>5</sup>, T. Unbehaun<sup>23</sup>, P. van der Merwe<sup>9</sup>, C. van Eldik<sup>23</sup>, B. van Soelen<sup>13</sup>, G. Vasileiadis<sup>29</sup>, M. Vecchi<sup>6</sup>, J. Veh<sup>23</sup>, C. Venter<sup>9</sup>, J. Vink<sup>36</sup>, H.J. Völk<sup>2</sup>, N. Vogel<sup>23</sup>, T. Wach<sup>23</sup>, S.J. Wagner<sup>4</sup>, F. Werner<sup>2</sup>, R. White<sup>2</sup>, A. Wierzcholska<sup>26</sup>, Yu Wun Wong<sup>23</sup>, H. Yassin<sup>9</sup>, M. Zacharias<sup>4,9</sup>, D. Zargaryan<sup>1</sup>, A.A. Zdziarski<sup>34</sup>, A. Zech<sup>20</sup>, S.J. Zhu<sup>11</sup>, A. Zmija<sup>23</sup>, S. Zouari<sup>15</sup> and N. Żywucka<sup>9</sup>.

<sup>1</sup>Dublin Institute for Advanced Studies, 31 Fitzwilliam Place, Dublin 2, Ireland

<sup>2</sup>Max-Planck-Institut für Kernphysik, P.O. Box 103980, D 69029 Heidelberg, Germany

<sup>3</sup>Yerevan State University, 1 Alek Manukyan St, Yerevan 0025, Armenia

<sup>4</sup>Landessternwarte, Universität Heidelberg, Königstuhl, D 69117 Heidelberg, Germany

<sup>5</sup>IRFU, CEA, Université Paris-Saclay, F-91191 Gif-sur-Yvette, France

<sup>6</sup>Kapteyn Astronomical Institute, University of Groningen, Landleven 12, 9747 AD Groningen, The Netherlands

<sup>7</sup>Laboratoire Leprince-Ringuet, École Polytechnique, CNRS, Institut Polytechnique de Paris, F-91128 Palaiseau, France

<sup>8</sup>University of Namibia, Department of Physics, Private Bag 13301, Windhoek 10005, Namibia

<sup>9</sup>Centre for Space Research, North-West University, Potchefstroom 2520, South Africa

<sup>10</sup>Universität Hamburg, Institut für Experimentalphysik, Luruper Chaussee 149, D 22761 Hamburg, Germany

<sup>11</sup>Deutsches Elektronen-Synchrotron DESY, Platanenallee 6, 15738 Zeuthen, Germany

<sup>12</sup>Obserwatorium Astronomiczne, Uniwersytet Jagielloński, ul. Orla 171, 30-244 Kraków, Poland

<sup>13</sup>Department of Physics, University of the Free State, PO Box 339, Bloemfontein 9300, South Africa

<sup>14</sup>Institut für Physik und Astronomie, Universität Potsdam, Karl-Liebknecht-Strasse 24/25, D 14476 Potsdam, Germany

<sup>15</sup>Université de Paris, CNRS, Astroparticule et Cosmologie, F-75013 Paris, France

<sup>16</sup>Department of Physics and Electrical Engineering, Linnaeus University, 351 95 Växjö, Sweden

<sup>17</sup>School of Physics, University of the Witwatersrand, 1 Jan Smuts Avenue, Braamfontein, Johannesburg, 2050 South Africa

<sup>18</sup>Institut für Physik, Humboldt-Universität zu Berlin, Newtonstr. 15, D 12489 Berlin, Germany

<sup>19</sup>Institut für Astronomie und Astrophysik, Universität Tübingen, Sand 1, D 72076 Tübingen, Germany

<sup>20</sup>Laboratoire Univers et Théories, Observatoire de Paris, Université PSL, CNRS, Université Paris Cité, 5 Pl. Jules Janssen, 92190 Meudon, France

<sup>21</sup>Sorbonne Université, Université Paris Diderot, Sorbonne Paris Cité, CNRS/IN2P3, Laboratoire de Physique Nucléaire et de Hautes Energies, LPNHE, 4 Place Jussieu, F-75252 Paris, France

<sup>22</sup>University of Oxford, Department of Physics, Denys Wilkinson Building, Keble Road, Oxford OX1 3RH, UK

<sup>23</sup>Friedrich-Alexander-Universität Erlangen-Nürnberg, Erlangen Centre for Astroparticle Physics, Nikolaus-Fiebiger-Str. 2, 91058 Erlangen, Germany

<sup>24</sup>Astronomical Observatory, The University of Warsaw, Al. Ujazdowskie 4, 00-478 Warsaw, Poland

<sup>25</sup>Université Savoie Mont Blanc, CNRS, Laboratoire d'Annecy de Physique des Particules - IN2P3, 74000 Annecy, France

<sup>26</sup>Instytut Fizyki Jądrowej PAN, ul. Radzikowskiego 152, 31-342 Kraków, Poland

<sup>27</sup>Université Bordeaux, CNRS, LP2I Bordeaux, UMR 5797, F-33170 Gradignan, France

<sup>28</sup>School of Physical Sciences, University of Adelaide, Adelaide 5005, Australia

<sup>29</sup>Laboratoire Univers et Particules de Montpellier, Université Montpellier, CNRS/IN2P3, CC 72, Place Eugène Bataillon, F-34095 Montpellier Cedex 5, France

<sup>30</sup>Aix Marseille Université, CNRS/IN2P3, CPPM, Marseille, France

<sup>31</sup>Universität Innsbruck, Institut für Astro- und Teilchenphysik, Technikerstraße 25, 6020 Innsbruck, Austria

<sup>32</sup>Institute of Astronomy, Faculty of Physics, Astronomy and Informatics, Nicolaus Copernicus University, Grudziadzka 5, 87-100 Torun, Poland

<sup>33</sup>Department of Physics, Rikkyo University, 3-34-1 Nishi-Ikebukuro, Toshima-ku, Tokyo 171-8501, Japan

<sup>34</sup>Nicolaus Copernicus Astronomical Center, Polish Academy of Sciences, ul. Bartycka 18, 00-716 Warsaw, Poland

<sup>35</sup>Department of Physics and Astronomy, The University of Leicester, University Road, Leicester, LE1 7RH, United Kingdom

<sup>36</sup>GRAPPA, Anton Pannekoek Institute for Astronomy, University of Amsterdam, Science Park 904, 1098 XH Amsterdam, The Netherlands

<sup>37</sup>Yerevan Physics Institute, 2 Alikhanian Brothers St., 0036 Yerevan, Armenia

<sup>38</sup>Department of Physics, Konan University, 8-9-1 Okamoto, Higashinada, Kobe, Hyogo 658-8501, Japan

<sup>39</sup>Kavli Institute for the Physics and Mathematics of the Universe (WPI), The University of Tokyo Institutes for Advanced Study (UTIAS), The University of Tokyo, 5-1-5 Kashiwa-no-Ha, Kashiwa, Chiba, 277-8583, Japan

<sup>40</sup>RIKEN, 2-1 Hirosawa, Wako, Saitama 351-0198, Japan